

Coalescence of complex fragments

B. V. Jacak, D. Fox, and G. D. Westfall

*National Superconducting Cyclotron Laboratory, Michigan State University,
East Lansing, Michigan 48824-1321*

(Received 29 October 1984)

The production of intermediate rapidity complex fragments up to $A=14$ from the reactions of Ar incident on Au and Ca targets at 92 and 137 MeV/nucleon has been described using the coalescence model. The resulting coalescence radii are independent of observed fragment mass which indicates that these fragments are emitted from a common source. Extracted interaction region radii agree with recent proton-proton correlation results.

The origins of light nuclei observed at intermediate rapidities from high energy nucleus-nucleus collisions are much less well understood than the emission of nucleons. The relative production cross sections and energy spectra of these fragments may carry signatures of various phenomena such as liquid-gas phase transitions^{1,2} or information concerning the state of the emitting system at different times during the evolution of the reaction.³⁻⁸ The production of light nuclei has been described in terms of the coalescence model,⁹⁻¹¹ chemical equilibrium models,¹⁰⁻¹³ intranuclear cascade calculations,^{14,15} and hydrodynamics coupled with thermal decay.⁷ The most successful is the coalescence model which has been applied to light particle spectra from nucleus-nucleus collisions ranging in incident energy from 9 MeV/nucleon to 2 GeV/nucleon.^{9-11,16} For the first time we have applied this model not only to light particles (d,t,³He,⁴He) but also to complex fragments ($6 \leq A \leq 14$) from intermediate energy nucleus-nucleus collisions.⁵ Surprisingly, the simple scaling relation predicted by this model is found to hold for fragments up to $A=14$. The extracted coalescence radii are independent of the observed fragment and incident energy and the interaction volume deduced from the coalescence radii agree with recent particle-particle correlation studies.¹⁷⁻¹⁹

In this model, composite fragments emitted from high energy nucleus-nucleus collisions are formed when nucleons are emitted close together in phase space. Nucleons within a specified momentum radius p_0 are assumed to coalesce into light nuclei while the rest are emitted as free nucleons. With the assumptions that the density of nucleons is considerably less than normal nuclear density, the proton and neutron spectra are identical in shape and the formation of light nuclei does not significantly deplete the original nucleon distribution, a simple scaling law is obtained where the composite fragment cross sections are obtained by raising the proton cross section to the power of the fragment mass number A . Invariably the simple scaling predicted by this model has been observed for light particles in spite of the fact that one or all of the preceding assumptions may not be satisfied.

The scaling relationship can be expressed as¹¹

$$E_A \left(\frac{d^3 \sigma_A}{dp_A^3} \right) = C_A \left[E_p \left(\frac{d^3 \sigma_p}{dp_p^3} \right) \right]^A, \quad (1)$$

where A is the fragment mass number, $d^3 \sigma_p / dp_p^3$ and $d^3 \sigma_A / dp_A^3$ are the proton and complex fragment momentum space densities, respectively, at the same velocity, E_p and E_A are the proton and fragment total energies, respectively,

and C_A is the scaling factor. The coalescence radius can be expressed as¹¹

$$p_0^3 = (3m\sigma_0/4\pi) \{C_A [(Z_t + Z_p)/(N_t + N_p)]^N A^2 N! Z!\}^{1/(A-1)}, \quad (2)$$

where N , N_t , and N_p are the fragment, target, and projectile

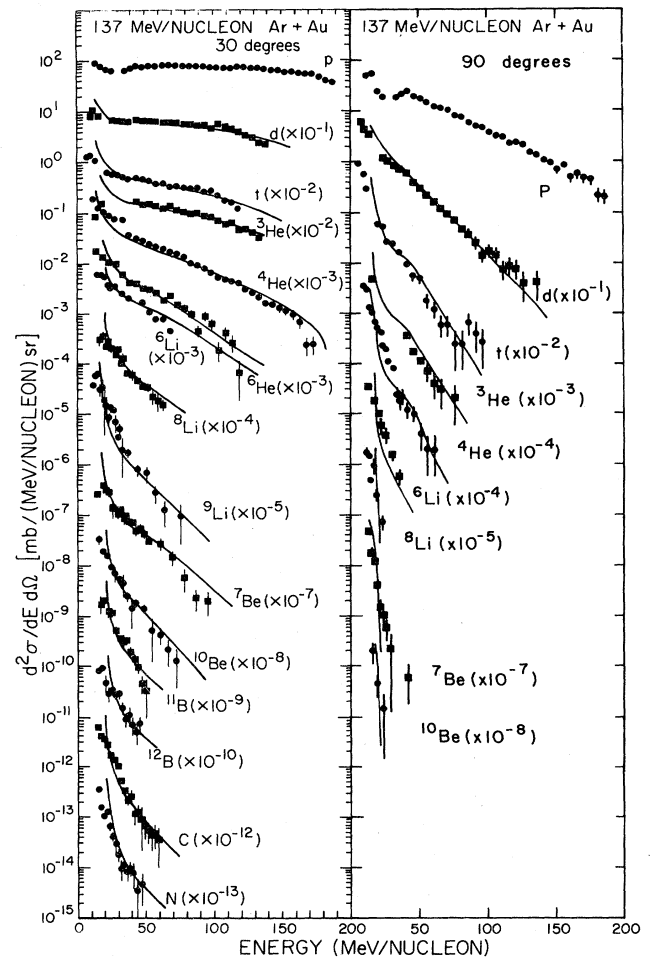


FIG. 1. Double differential cross section for fragments from 137 MeV/nucleon Ar+Au at 30° and 90° (Ref. 5). Not all the fragments are shown. The solid lines correspond to coalescence model fits as described in the text.

neutron numbers, respectively, Z , Z_t , and Z_p are the fragment, target, and projectile proton numbers, respectively, m is the nucleon rest mass, and σ_0 is the geometric reaction cross section with $r_0 = 1.2$ fm.

The data we wish to describe using this formulation are energy spectra of light particles and complex fragments from the reactions of 92 and 137 MeV/nucleon Ar+Ca and Au.⁵ Representative energy spectra at 30° and 90° for Ar+Au are presented in Fig. 1. The different symbols represent the observed energy spectra for a given particle. The angles and particles that are not shown follow the trends demonstrated by the angles and particles shown in this figure. An example of the complete angular distribution of spectra for ⁷Be is given in Fig. 2. The solid lines in both figures represent the proton energy spectra at the same energy/nucleon in the laboratory raised to the A th power as described above. The normalization of each curve is the same for all angles for a given particle and leads directly to the extraction of the coalescence radius for that particle from each type of reaction using Eqs. (1) and (2). The resulting coalescence radii are plotted in Fig. 3 as a function of fragment mass for two incident Ar energies, 92 and 137 MeV/nucleon, and two targets, Ca and Au.

In Fig. 3 one can see that the coalescence radii are independent of the fragment mass and, within errors, the coalescence radii are constant with fragment mass although there is an apparent trend toward higher values above $A = 8$. Statistically the values from both energies for each target can be described by one value of the coalescence radius, $p_0 = 157.2$ MeV/ c for Ar+Ca and 154.7 MeV/ c for Ar+Au. This constancy can be interpreted as evidence that these fragments are all emitted from a common source and is in agreement with the result of single moving source fits where these fragments were also described with a consistent

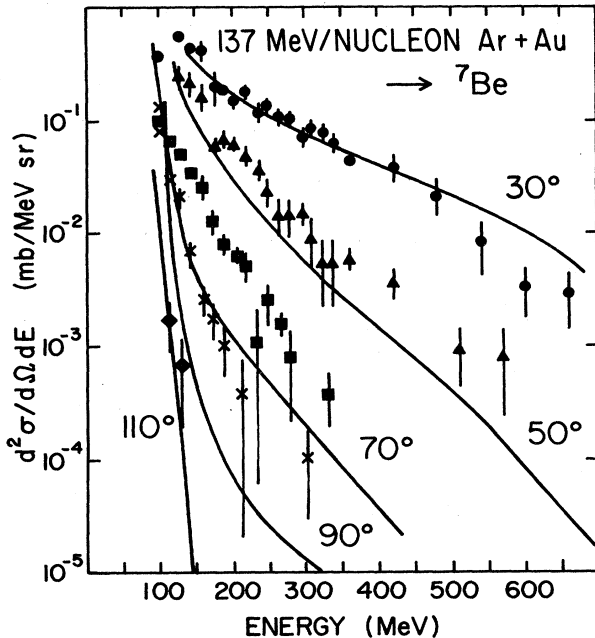


FIG. 2. Double differential cross sections for 137 MeV/nucleon Ar+Au leading to ⁷Be (Ref. 5). The solid lines are coalescence model fits as described in the text.

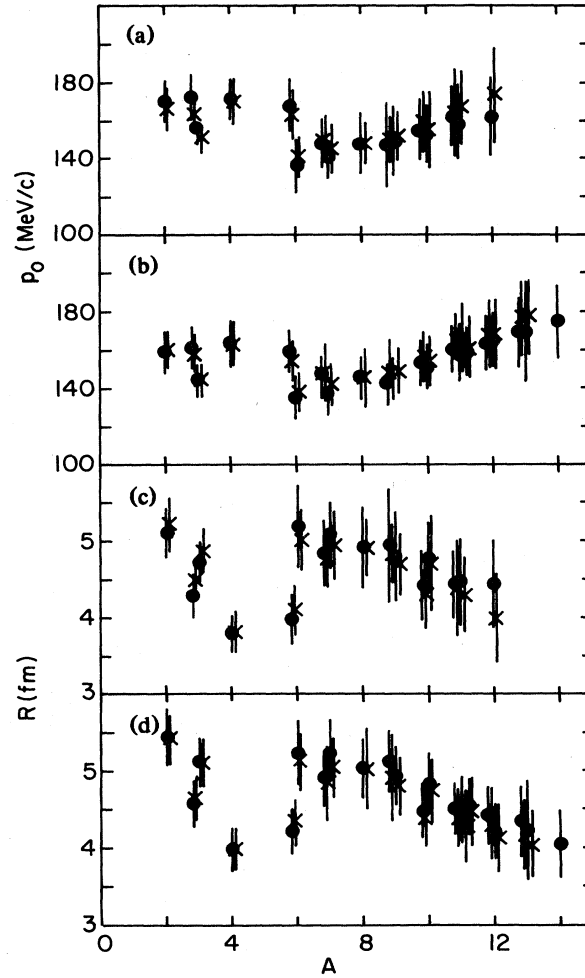


FIG. 3. (a) Coalescence radii p_0 for Ar+Ca, (b) coalescence radii for Ar+Au, (c) interaction volume radii R for Ar+Ca, (d) interaction volume radii for Ar+Au. Circles and crosses represent the 137 and 92 MeV/nucleon incident energies cases, respectively.

set of parameters within a thermal model framework.⁵

One can relate the extracted coalescence radius to the rms radius of the interaction zone between the target and projectile nuclei R using the following formulation:¹²

$$R^3 = (Z!N!)^{1/(A-1)} (9h^3/16\pi^2 \bar{p}_0^3) , \quad (3)$$

where \bar{p}_0 is the reduced coalescence radius defined as¹²

$$\bar{p}_0^3 = \{ [2^A / [A^3 (2S_A + 1)]]^{1/(A-1)} \} p_0^3 \quad (4)$$

and S_A is the ground state spin of the fragment. The interaction radii are shown in Fig. 3 along with the coalescence radii as a function of observed fragment mass number. The radii are statistically consistent with a constant value of 4.5 and 4.7 fm for Ar+Ca and Ar+Au, respectively, although the trend for the heavier fragments is toward smaller radii. Thus, the two systems appear to have a similar number of participant nucleons despite the fact that a participant-spectator geometry calculation predicts that the impact parameter averaged interaction volumes should differ by a factor of 2. The radii extracted using light parti-

cles decrease with increasing mass as was observed in Ref. 11. However, this decrease does not continue with heavier masses and implies that the extraction of interaction volume radii using this formulation must include complex fragments as well as light particles.

The present results for interaction volume radii agree roughly with the results¹⁹ for 400 MeV/nucleon Nb+Nb and Ca+Ca using the Plastic Ball. In that work the interaction volume was measured using two-proton correlations as a function of the observed charged particle multiplicity. However, the observed radius was almost constant above a multiplicity of 10 with $R \approx 4$ fm for Ca+Ca and $R \approx 5$ fm for Nb+Nb. Because the present analysis deals with complex fragments emitted at intermediate rapidities, the results must be biased toward central collisions and indeed the interaction volume is similar to that found using the high multiplicity selected data in Ref. 19. Other particle correlation measurements have yielded similar interaction radii for multiplicity averaged data. A proton-proton correlation measurement¹⁸ for 25 MeV/nucleon O+Au obtained $R \approx 5$ fm (≈ 4 fm Gaussian) while a two pion correlation measurement¹⁷ for 1.5 GeV/nucleon Ar+KCl yielded

$R = 6.0 \pm 0.6$ fm (4.9 ± 0.5 fm Gaussian).

In summary, we have found that not only can the production of light nuclei from high energy nucleus-nucleus collisions described by the coalescence model, but that intermediate rapidity complex fragments up to $A = 14$ can be described as well. The resulting coalescence radii are independent of fragment mass and lead to values of the radii of the interaction volume that agree with the results of two-proton correlation measurements but are somewhat lower than the pion-pion correlation results. Measuring these fragments is much like performing a multiparticle correlation experiment except that both charged particles and neutrons bound in the fragments are included and only inclusive cross sections are measured. The extracted interaction volumes for Ar+Ca and Ar+Au are nearly the same, which argues against the spectator-participant geometry which predicts that the two cases should be different by a factor of 2.

The authors thank W. Benenson and H. Stöcker for helpful comments. This work was supported by the National Science Foundation under Grant No. PHY-83-12245.

-
- ¹H. Schulz, L. Münchow, G. Röpker, and M. Schmidt, Phys. Lett. **119B**, 12 (1982).
²M. W. Curtin, H. Toki, and D. K. Scott, Phys. Lett. **123B**, 289 (1983).
³A. Mekjian, Phys. Rev. Lett. **38**, 640 (1977).
⁴P. J. Siemens and J. I. Kapusta, Phys. Rev. Lett. **43**, 1486 (1979).
⁵B. V. Jacak, G. D. Westfall, C. K. Gelbke, L. H. Harwood, W. G. Lynch, D. K. Scott, H. Stöcker, M. B. Tsang, and T. J. M. Symons, Phys. Rev. Lett. **51**, 1846 (1983).
⁶B. V. Jacak, H. Stöcker, and G. D. Westfall, Phys. Rev. C **29**, 1744 (1984).
⁷H. Stöcker, G. Buchwald, G. Graebner, P. Subramanian, J. A. Maruhn, W. Greiner, B. V. Jacak, and G. D. Westfall, Nucl. Phys. **A400**, 63c (1983).
⁸D. J. Morrissey, W. Benenson, E. Kashy, B. Sherrill, A. D. Panagiotou, R. A. Blue, R. M. Ronningen, J. van der Plicht, and H. Utsunomiya, Phys. Lett. **148B**, 423 (1984).
⁹H. H. Gutbrod, A. Sandoval, P. J. Johansen, A. M. Poskanzer, J. Gosset, W. G. Meyer, G. D. Westfall, and R. Stock, Phys. Rev. Lett. **37**, 667 (1976).
¹⁰J. Gosset, H. H. Gutbrod, W. G. Meyer, A. M. Poskanzer, A. Sandoval, R. Stock, and G. D. Westfall, Phys. Rev. C **16**, 629 (1977).
¹¹M.-C. Lemaire, S. Nagamiya, S. Schnetzer, H. Steiner, and I. Tanihata, Phys. Lett. **85B**, 38 (1979).
¹²A. Mekjian, Phys. Rev. C **17**, 1051 (1978).
¹³J. Gosset, J. I. Kapusta, and G. D. Westfall, Phys. Rev. C **18**, 844 (1978).
¹⁴V. D. Toneev and K. K. Gudima, Nucl. Phys. **A400**, 173c (1983).
¹⁵H. Kruse, B. V. Jacak, G. D. Westfall, and H. Stöcker (unpublished).
¹⁶T. C. Awes, S. Saini, G. Poggi, C. K. Gelbke, D. Cha, R. Legrain, and G. D. Westfall, Phys. Rev. C **25**, 2361 (1982).
¹⁷D. Beavis, S. Y. Fung, W. Gorn, A. Huie, D. Keane, J. J. Lu, R. T. Poe, B. C. Shen, and G. VanDalen, Phys. Rev. C **27**, 910 (1983).
¹⁸W. G. Lynch, C. B. Chitwood, M. B. Tsang, D. J. Fields, D. R. Klesch, C. K. Gelbke, G. R. Young, T. C. Awes, R. L. Ferguson, F. E. Obershein, F. Plasil, R. L. Robinson, and A. D. Panagiotou, Phys. Rev. Lett. **51**, 1850 (1983).
¹⁹H. A. Gustafsson, H. H. Gutbrod, B. Kolb, H. Löhner, B. Ludewigt, A. M. Poskanzer, T. Renner, H. Riedesel, H. G. Ritter, A. Warwick, F. Weik, and H. Wieman, Phys. Rev. Lett. **53**, 544 (1984).